Aust. J. Phys., 1996, **49**, 301–19

Spin-resolved Alignment and Orientation Effects in Atomic Collisions*

Klaus Bartschat[A] *and Nils Andersen*[B]

[A] Department of Physics and Astronomy, Drake University, Des Moines, IA 50311, USA.
[B] Niels Bohr Institute, Ørsted Laboratory, Universitetsparken 5, DK-2100 Copenhagen, Denmark.

Abstract

The density matrix parametrisation of collisionally excited atomic ensembles is generalised to account for projectile and target spin polarisations. The density matrix elements, containing spin-resolved alignment and orientation parameters, can be determined by measurements of the 'generalised Stokes parameters' introduced by Andersen and Bartschat (1994) to describe scattered-projectile–polarised-photon coincidence experiments. Focusing on electron impact excitation of light alkali-type targets and mercury, the present experimental status of such experiments is reviewed, in particular with regard to the 'perfect scattering experiment' whereby all independent scattering amplitudes are determined.

1. Introduction

Scattered-electron–polarised-photon coincidence studies are well known to provide some of the most detailed tests of atomic collision models to date. Most experiments so far have been performed without spin preparation in the initial state and projectile spin analysis in the final state (for recent reviews, see Andersen *et al.* 1988; Becker *et al.* 1992), with the most notable exceptions being the time-reversed superelastic e–Na studies of the NIST group (see, for example, McClelland *et al.* 1989; Kelley *et al.* 1992) and the work of Goeke *et al.* (1988, 1989) and of Sohn and Hanne (1992) who reported results using polarised incident electrons for excitation of the $(6s^2)^1S_0 \rightarrow (6s6p)^3P_1$ transition in Hg. For an introduction to polarised electron physics, we refer to the book by Kessler (1985).

On the theoretical side, the general theory of electron–photon coincidence experiments using spin-polarised electron beams has been outlined by Bartschat *et al.* (1981) who provided explicit formulae for the state multipoles describing the atomic density matrix of an excited state with total angular momentum $J = 1$ and odd parity, as well as general equations for the Stokes parameters that determine the polarisation state of the emitted photons in the optical decay of such a state. In their paper, Bartschat *et al.* used the 'collision frame', i.e. the quantisation axis z^c was chosen along the incident beam direction and the y^c-axis was defined to be perpendicular to the scattering plane. While this system is

* Refereed paper based on a contribution to the Advanced Workshop on Atomic and Molecular Physics, held at the Australian National University, Canberra, in February 1995.

0004-9506/96/020301$10.00

standard for numerical calculations, the general formulae become, unfortunately, rather cumbersome.

In a well-known review, Andersen *et al.* (1988) used the 'natural coordinate frame' with the quantisation axis z^n chosen perpendicular to the scattering plane and the incident beam direction defining the axis x^n to set the framework for unpolarised electron–photon coincidence studies, a framework that has by now become the standard formulation in this field of collision physics. In light of the success of their parametrisation, which allows for intuitive interpretation of the density matrix parameters describing the excited atomic ensemble, we recently extended the formulation to the cases of spin-polarised electron impact excitation of spin-polarised alkali-type targets such as hydrogen and sodium (Andersen and Bartschat 1993, to be referred to as I below), as well as heavy quasi two-electron systems such as mercury (Andersen and Bartschat 1994, to be referred to as II below). A specialised analysis for the electron–sodium experiment of the NIST group using this coordinate frame was already given by Hertel *et al.* (1987).

In this paper, we present a systematic overview of the increasing complexity that arises in the description of electron impact excitation processes when one goes from light targets without orbital or spin angular momentum in the initial state (like helium) to light hydrogen, or alkali-like, targets with non-vanishing spins and, finally, to heavy targets (such as mercury) where explicitly spin–dependent effects like the spin-orbit interaction must be taken into account, both in the general formulation and in numerical calculations. Spin-resolved density matrix parametrisations are given, and it is shown how the various parameters can be determined from the "generalised Stokes parameters" introduced in II. Furthermore, it is pointed out that the "generalised *STU* parameters" (Bartschat 1989), which describe the change of the projectile spin polarisation during the collision, sometimes contain equivalent information that can be used for consistency checks or, in other cases, completely new information that is needed for a "perfect scattering experiment". Such experiments, in which all independent scattering amplitudes are determined, were first called for by Bederson (1970). Data from perfect experiments, if available, provide the most detailed comparison between experiment and theory, since they contain no more averaging over key variables like impact parameter, magnetic quantum numbers, or electron spin. Such averaging may partly or completely obscure the collision dynamics and makes comparison between theory and experiment less valuable.

For many fundamental processes the focus of investigation has, therefore, increasingly been concentrated on identifying dimensionless quantities which can be derived from relative intensity measurements. The study of such quantities, termed alignment and orientation parameters, has by now reached a very high level of sophistication. Although the goal of "perfect" has presently been achieved in a few cases only, this approach has dramatically increased our understanding of the collision dynamics for a broad range of collision processes.

This paper is organised as follows. In Section 2, we briefly review the general description of excited atomic P states, as given by Andersen *et al.* (1988) for unpolarised beam experiments. We then present some basic experimental schemes that have been used with spin-polarised beams. Section 3 deals with the density matrix parametrisation for various cases of interest, with a systematic increase in complexity for the target systems mentioned above. We will restrict the

discussion to P states and use the "natural coordinate system" unless otherwise indicated. Sections 4 and 5 summarise the basic ideas behind the "generalised Stokes" and the "generalised *STU* parameters" from which various density matrix elements can be extracted, and the "completeness" of experimental investigations is discussed in Section 6. The results are illustrated in Section 7 where a comparison of experimental data with theoretical predictions allows for a critical assessment of the present situation. A summary is given in Section 8, followed by suggestions for future work in this area. For a more comprehensive evaluation of the field, we refer to a forthcoming review (Andersen *et al.* 1996*a*).

2. Collisionally Excited P states and Their Experimental Investigation

As shown by Andersen *et al.* (1988), an atomic ensemble in collisionally excited P states, as created in unpolarised beam experiments, can be fully described in terms of three independent parameters, namely the alignment angle γ, the angular momentum transfer $L_\perp$, and the height of the charge cloud h. The latter parameter, however, must vanish unless the atomic reflection symmetry is violated. This may happen, for example, if spin-flips caused by the spin–orbit interaction take place during the collision process; spin-flips by exchange alone do not result in a finite height of the charge cloud. An example is shown in Fig. 1.

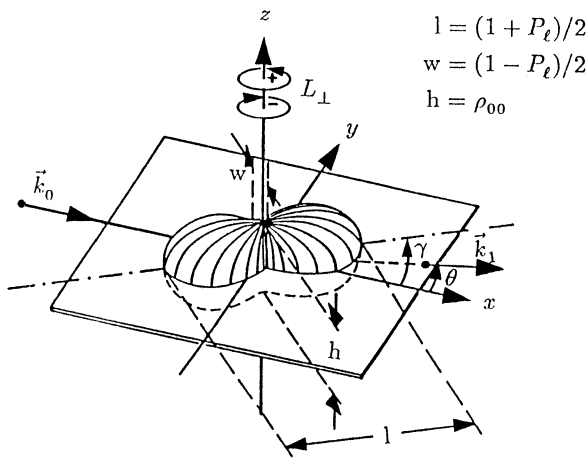

Fig. 1. Schematic diagram of a collisionally induced charge cloud of an atom excited to a P state by impact of a particle with incident momentum $\mathbf{k}_0$ and final momentum $\mathbf{k}_1$, scattered at an angle θ. (From Andersen *et al.* 1988.)

The charge cloud parameters can be determined from the pattern of the emitted dipole radiation in electron–photon coincidence experiments. Only in exceptional cases, however, such as He 2^1P and 3^3P excitation, is a "perfect experiment" possible with unpolarised beams. Alternatively, the equivalent information may be obtained from the "time-reversed" superelastic scheme where de-excitation of laser-excited atomic ensembles is studied. The latter arrangement was pioneered by the NIST group (McClelland *et al.* 1985, 1989) who used the laser-pumping process to produce a spin-polarised atomic beam. Spin-polarised electron beams are routinely obtained from GaAs sources (Pierce *et al.* 1980) and have been used

both in the NIST superelastic setups as well as in electron–photon coincidence experiments conducted by the Münster group (Goeke *et al.* 1989; Sohn and Hanne 1992, and references therein). The basic schemes of the two arrangements are illustrated in Fig. 2.

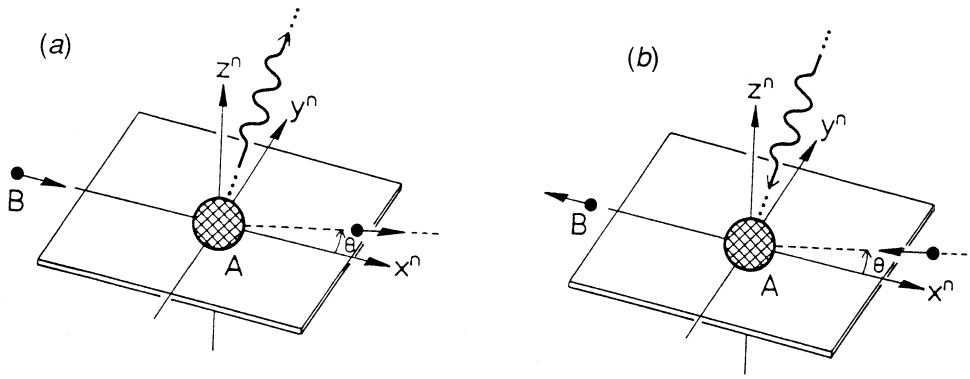

Fig. 2. Study possibilities of the process shown in Fig. 1. (*a*) Photons emitted in the P → S decay are polarisation analysed (Stokes parameters) in a selected direction, and detected in coincidence with the scattered particle. (*b*) In the time-reversed scheme, the atom A is excited by photons coming in from a selected direction, and the number of particles B leading to de-excitation are detected as a function of laser polarisation. The two approaches yield essentially equivalent information.

3. Scattering Amplitudes and Density Matrix Parametrisation

In general, transitions from an initial state $|J_i M_i; \mathbf{k}_i m_i\rangle$ to a final state $|J_f M_f; \mathbf{k}_f m_f\rangle$ are described by the scattering amplitudes

$$f(M_f m_f; M_i m_i; \theta) = \langle J_f M_f; \mathbf{k}_f m_f \mid \mathcal{T} \mid J_i M_i; \mathbf{k}_i m_i \rangle \,, \tag{1}$$

where $\mathcal{T}$ is the transition operator. Furthermore, $J_i\,(J_f)$ is the total electronic angular momentum in the initial (final) state of the target and $M_i\,(M_f)$ its corresponding z-component, while $k_i\,(k_f)$ is the initial (final) momentum of the projectile and $m_i\,(m_f)$ its spin component. The scattering angle θ is the angle between $\mathbf{k}_i$ and $\mathbf{k}_f$.

There are, in general, $4(2J_i{+}1)(2J_f{+}1)$ possible combinations of magnetic quantum numbers. Due to parity conservation of all interactions determining the outcome of the collision process, the number of independent scattering amplitudes is cut in half, giving a total of $2(2J_i+1)(2J_f+1)$ *complex* amplitudes for each transition between fine-structure levels. The total number of independent *real* parameters is thus $4(2J_i{+}1)(2J_f{+}1){-}1$, taking into account the common, arbitrary phase. These are usually parametrised as one *absolute* differential cross section and $4(2J_i+1)(2J_f+1)-2$ *dimensionless* numbers, namely $2(2J_i+1)(2J_f+1)-1$ relative magnitudes and $2(2J_i+1)(2J_f+1)-1$ relative phases.

The number of independent scattering amplitudes, however, is often drastically reduced if relativistic effects may be neglected during the collision process. This is usually the case for transitions involving outer-shell electrons in light target atoms and results in conservation theorems for the total orbital angular momentum $\bar{L}$ and the total spin $\bar{S}$ of the combined projectile + target system separately.

Consequently, the transition $He(1s^2)^1S \longrightarrow He(1s2p)^1P$ can be described by only two amplitudes, f_{+1} and f_{-1} with relative phase δ (see Fig. 3), while the transitions $H(1s)^2S \longrightarrow H(2p)^2P$ or $Na(3s)^2S \longrightarrow Na(3p)^2P$ require four amplitudes, namely $f_{+1}^{s,t}$ and $f_{-1}^{s,t}$. In the latter case, the superscripts "s" and "t" stand for singlet and triplet total spin channels, respectively. The subscripts "± 1" denote the magnetic quantum number of the excited P state. Note that the amplitudes for excitation of $M_L = 0$ vanish for these light targets, due to the conservation of the total spin which, in turn, corresponds to conservation of atomic reflection symmetry. On the other hand, the transition $Hg(6s^2)^1S_0 \longrightarrow (6s6p)^3P_1$ is described by six independent amplitudes, $f_{+1}^{\uparrow,\downarrow}$, $f_0^{\uparrow,\downarrow}$ and $f_{-1}^{\uparrow,\downarrow}$ where the superscripts "$\uparrow$, $\downarrow$" denote the spin projection of the incident electron. Conservation of the total (orbital + spin) electronic angular momentum $\bar{J}$ and its component $\bar{M}_J$ allows for the prediction of the spin component of the outgoing electron for each amplitude. As shown in II, the electron spin component remains unchanged for excitation of magnetic sublevels with $M_J = \pm 1$ while the spin is flipped if the $M_J = 0$ sublevel is excited. These spin-flips are, therefore, responsible for a non-vanishing cross section $\sigma(M_J{=}0)$ and lead to a finite height of the atomic charge cloud. Specifically, $h = \rho_{00} = \sigma(0)/\sigma_u$ where σ_u is the differential cross section for unpolarised beams, summed over all magnetic sublevels.

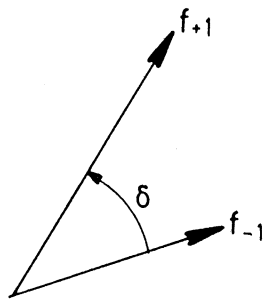

Fig. 3. Schematic diagram of scattering amplitudes in the natural frame for S → P transitions by electron impact without inclusion of electron spin.

While the scattering amplitudes are the central elements in numerical calculations, they do not appear individually in the description of practical experiments. Observables can only be expressed as bilinear product combinations of complex scattering amplitudes, subject to the following two restrictions that often need to be taken into account: (i) there is no "pure" initial state, and (ii) not all possible quantum numbers are simultaneously determined in the final state.

The density matrix formalism provides a systematic tool for handling these situations. To set up the notation, we recall that the density matrix of an excited P state for unpolarised beam experiments with conservation of atomic reflection symmetry can be written as (for details see Andersen *et al.* 1988)

$$\rho = \sigma \, \frac{1}{2} \begin{pmatrix} 1 + L_\perp & 0 & -P_\ell e^{-2i\gamma} \\ 0 & 0 & 0 \\ -P_\ell e^{2i\gamma} & 0 & 1 - L_\perp \end{pmatrix} . \qquad (2)$$

The angular momentum transfer is defined by

$$L_\perp = \frac{|f_{+1}|^2 - |f_{-1}|^2}{|f_{+1}|^2 + |f_{-1}|^2} = \frac{|f_{+1}|^2 - |f_{-1}|^2}{\sigma} \tag{3}$$

and the alignment angle γ is related to the phase difference δ between the two amplitudes $f_{\pm 1}$ through

$$\delta = -2\gamma + \pi \,. \tag{4}$$

The situation becomes more complicated for the case where the target atom has a non-vanishing spin and spin-flips, by exchange only, are possible. As long as the atomic reflection symmetry is still conserved, the density matrix for unpolarised beam experiments can be decomposed as follows (for details, see I):

$$\rho_u = \sigma_u \, \tfrac{1}{2} \begin{pmatrix} 1 + L_\perp & 0 & -P_\ell \, \mathrm{e}^{-2\,i\,\gamma} \\ 0 & 0 & 0 \\ -P_\ell \, \mathrm{e}^{2\,i\,\gamma} & 0 & 1 - L_\perp \end{pmatrix} \tag{5}$$

$$= 3w^t \, \sigma_u \, \tfrac{1}{2} \begin{pmatrix} 1 + L_\perp^t & 0 & -P_\ell^t \, \mathrm{e}^{-2\,i\,\gamma^t} \\ 0 & 0 & 0 \\ -P_\ell^t \, \mathrm{e}^{2\,i\,\gamma^t} & 0 & 1 - L_\perp^t \end{pmatrix}$$

$$+ w^s \, \sigma_u \, \tfrac{1}{2} \begin{pmatrix} 1 + L_\perp^s & 0 & -P_\ell^s \, \mathrm{e}^{-2\,i\,\gamma^s} \\ 0 & 0 & 0 \\ -P_\ell^s \, \mathrm{e}^{2\,i\,\gamma^s} & 0 & 1 - L_\perp^s \end{pmatrix} \tag{6}$$

There are now spin-dependent angular momentum transfers and alignment angles, as well as weight parameters w^t and w^s that determine the relative importance of the triplet and the singlet spin channels, respectively. For symmetry reasons, we prefer these weights over the parameter $r = \sigma^t/\sigma^s$ that denotes the ratio of the triplet and the singlet cross sections. These parameters are related as follows (for details see Andersen *et al.* 1996*b*):

$$w^t = \frac{\sigma^t}{\sigma^s + 3\sigma^t} = \frac{\sigma^t}{4\sigma_u} \,, \tag{7}$$

$$w^s = \frac{\sigma^s}{\sigma^s + 3\sigma^t} = \frac{\sigma^s}{4\sigma_u} = 1 - 3w^t \,, \tag{8}$$

$$\sigma_u = \tfrac{3}{4}\,\sigma^t + \tfrac{1}{4}\,\sigma^s \,, \tag{9}$$

$$r = \frac{w^t}{1 - 3w^t} \,, \tag{10}$$

where σ_u is the differential cross section for unpolarised beams.

Finally, the complexity increases even further if the atomic reflection symmetry is not conserved any longer. Consider, for example, a $J_0 = 0 \longrightarrow J_1 = 1$ transition, such as $(6s^2)^1S_0 \longrightarrow (6s6p)^3P_1$ in mercury. If one restricts the electron polarisation to be perpendicular to the scattering plane, i.e. $\mathbf{P} = P\hat{\mathbf{z}}$, the density matrix for unpolarised beam excitation can be de-composed as (Andersen *et al.* 1996*b*)

$$\rho_u = \sigma_u \left[(1-h)\,\tfrac{1}{2} \begin{pmatrix} 1+L_\perp^+ & 0 & -P_\ell^+ \, \mathrm{e}^{-2i\gamma} \\ 0 & 0 & 0 \\ -P_\ell^+ \, \mathrm{e}^{2i\gamma} & 0 & 1-L_\perp^+ \end{pmatrix} + h \begin{pmatrix} 0 & 0 & 0 \\ 0 & 1 & 0 \\ 0 & 0 & 0 \end{pmatrix} \right] \tag{11}$$

$$= w^\uparrow \sigma_u \left[(1-h^\uparrow)\,\tfrac{1}{2} \begin{pmatrix} 1+L_\perp^{+\uparrow} & 0 & -P_\ell^{+\uparrow} \, \mathrm{e}^{-2i\gamma^\uparrow} \\ 0 & 0 & 0 \\ -P_\ell^{+\uparrow} \, \mathrm{e}^{2i\gamma^\uparrow} & 0 & 1-L_\perp^{+\uparrow} \end{pmatrix} + h^\uparrow \begin{pmatrix} 0 & 0 & 0 \\ 0 & 1 & 0 \\ 0 & 0 & 0 \end{pmatrix} \right]$$

$$+ w^\downarrow \sigma_u \left[(1-h^\downarrow)\,\tfrac{1}{2} \begin{pmatrix} 1+L_\perp^{+\downarrow} & 0 & -P_\ell^{+\downarrow} \, \mathrm{e}^{-2i\gamma^\downarrow} \\ 0 & 0 & 0 \\ -P_\ell^{+\downarrow} \, \mathrm{e}^{2i\gamma^\downarrow} & 0 & 1-L_\perp^{+\downarrow} \end{pmatrix} + h^\downarrow \begin{pmatrix} 0 & 0 & 0 \\ 0 & 1 & 0 \\ 0 & 0 & 0 \end{pmatrix} \right] \tag{12}$$

The alignment, orientation and height parameters now depend on the spin projection of the incident electron, and weighting factors $w^\uparrow = 1 - w^\downarrow$ determine the relative cross sections for these spin components.

4. Generalised Stokes Parameters

The density matrix elements defined above can be determined in electron–photon coincidence experiments or, equivalently, with the "time-reversed" superelastic scattering setup. Fig. 4 shows the definition of the "generalised Stokes parameters" that we introduced in II. They are defined in such a way that all four possible combinations of photon polarisation analyser and initial electron polarisations are present on an equal footing. (Instead of the photon analyser, the laser polarisation would have to be switched in the superelastic setup.)

We first introduce the following notation: The quantity $I^{\hat{\mathbf{n}}}_{\pm P_{x,y,z}}(\beta)$ is the light intensity transmitted by a linear polarisation analyser oriented at an angle β for incident electron polarisations in the x, y or z direction, with the light being observed in the direction denoted by $\hat{\mathbf{n}}$. Similar definitions are made for the intensities transmitted by circular polarisation analysers. With P_1 denoting the standard first Stokes parameter, this gives, for example:

$$I^{\hat{\mathbf{n}}}_{\pm P_z}(0°) = \tfrac{1}{2}\,[I^{\hat{\mathbf{n}}}_{\pm P_z} + (IP_1)^{\hat{\mathbf{n}}}_{\pm P_z}]\,, \tag{13}$$

$$I^{\hat{\mathbf{n}}}_{\pm P_z}(90°) = \tfrac{1}{2}\,[I^{\hat{\mathbf{n}}}_{\pm P_z} - (IP_1)^{\hat{\mathbf{n}}}_{\pm P_z}]\,, \tag{14}$$

and the total intensity for unpolarised incident electrons can be constructed as

$$I_u^{\hat{\mathbf{n}}} = \tfrac{1}{4}\left[I_{+P_z}^{\hat{\mathbf{n}}}(0°) + I_{-P_z}^{\hat{\mathbf{n}}}(0°) + I_{+P_z}^{\hat{\mathbf{n}}}(90°) + I_{-P_z}^{\hat{\mathbf{n}}}(90°)\right] . \tag{15}$$

We then define the "generalised Stokes parameters" by taking the three other independent (except for a trivial sign) linear combinations of the four intensities. Specifically, we use

$$Q_{1,P_{x,y,z}}^{\hat{\mathbf{n}},++--} \equiv \frac{I_{+P_{x,y,z}}^{\hat{\mathbf{n}}}(0°) + I_{-P_{x,y,z}}^{\hat{\mathbf{n}}}(0°) - I_{+P_{x,y,z}}^{\hat{\mathbf{n}}}(90°) - I_{-P_{x,y,z}}^{\hat{\mathbf{n}}}(90°)}{I_{+P_{x,y,z}}^{\hat{\mathbf{n}}}(0°) + I_{-P_{x,y,z}}^{\hat{\mathbf{n}}}(0°) + I_{+P_{x,y,z}}^{\hat{\mathbf{n}}}(90°) + I_{-P_{x,y,z}}^{\hat{\mathbf{n}}}(90°)} , \tag{16}$$

$$Q_{1,P_{x,y,z}}^{\hat{\mathbf{n}},+--+} \equiv \frac{I_{+P_{x,y,z}}^{\hat{\mathbf{n}}}(0°) - I_{-P_{x,y,z}}^{\hat{\mathbf{n}}}(0°) - I_{+P_{x,y,z}}^{\hat{\mathbf{n}}}(90°) + I_{-P_{x,y,z}}^{\hat{\mathbf{n}}}(90°)}{I_{+P_{x,y,z}}^{\hat{\mathbf{n}}}(0°) + I_{-P_{x,y,z}}^{\hat{\mathbf{n}}}(0°) + I_{+P_{x,y,z}}^{\hat{\mathbf{n}}}(90°) + I_{-P_{x,y,z}}^{\hat{\mathbf{n}}}(90°)} , \tag{17}$$

$$Q_{1,P_{x,y,z}}^{\hat{\mathbf{n}},+-+-} \equiv \frac{I_{+P_{x,y,z}}^{\hat{\mathbf{n}}}(0°) - I_{-P_{x,y,z}}^{\hat{\mathbf{n}}}(0°) + I_{+P_{x,y,z}}^{\hat{\mathbf{n}}}(90°) - I_{-P_{x,y,z}}^{\hat{\mathbf{n}}}(90°)}{I_{+P_{x,y,z}}^{\hat{\mathbf{n}}}(0°) + I_{-P_{x,y,z}}^{\hat{\mathbf{n}}}(0°) + I_{+P_{x,y,z}}^{\hat{\mathbf{n}}}(90°) + I_{-P_{x,y,z}}^{\hat{\mathbf{n}}}(90°)} . \tag{18}$$

Similar definitions are made for the subscripts "2" and "3" where the analyser settings $(0°, 90°)$ are replaced by $(45°, 135°)$ and (RHC, LHC), respectively. This results in a Stokes parameter matrix for each direction of observation, with the first row corresponding to equations (16)–(18).

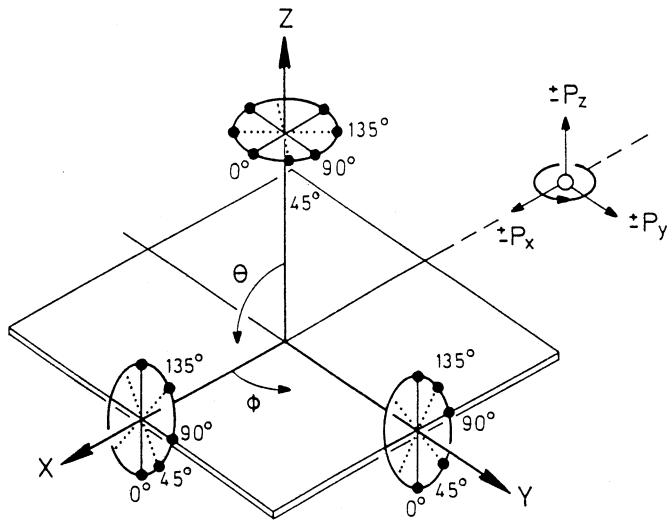

Fig. 4. Coordinate frame for definition of generalised Stokes parameters. The linear polariser settings in the directions $\hat{\mathbf{n}} = x, y, z$ are shown for polariser angles $\beta = 0°, 45°, 90°$ and $135°$, following the notation of Blum (1981). The incident polarised electron beam is characterised by polarisations $\pm P_x, \pm P_y$ or $\pm P_z$, as indicated.

Note that the first column of the generalised Stokes parameter matrix, i.e. the parameters $\left(Q_i^{\hat{\mathbf{n}},++--}\right)_{\mathbf{P}} \equiv \left(Q_{i1}^{\hat{\mathbf{n}}}\right)_{\mathbf{P}}$, $i = \{1, 2, 3\}$, is the standard Stokes vector (P_1, P_2, P_3) for unpolarised incident electrons. Similarly, the parameters in

the third column $\left(Q_i^{\hat{\mathbf{z}},+-+-}\right)_{\mathbf{P}} \equiv \left(Q_{i3}^{\hat{\mathbf{z}}}\right)_{\mathbf{P}}$ correspond to an "optical asymmetry" which compares light intensities measured with spin-up and spin-down electrons, independent of the light analyser setting. Consequently, measurements of the first column with different electron polarisations and of the third column with different light analyser settings *should*, in principle, yield the same result. Such measurements can thus provide valuable consistency checks in these highly sophisticated experiments and assist, for example, in the search for purely instrumental asymmetries.

As a well-known example for the determination of density matrix elements from the Stokes parameters of the emitted radiation, we recall that the two independent parameters $L_\perp$ and γ defined in equations (3) and (4) for electron impact excitation of helium-like systems can be obtained from the standard Stokes vector for light detected perpendicular to the scattering plane as follows:

$$P_1 + i\,P_2 = P_\ell\; e^{2i\gamma} = -\frac{2}{\sigma}\,|f_{+1}|\,|f_{-1}|\,\mathrm{e}^{-i\delta}\,, \tag{19}$$

$$P_3 = -L_\perp\,. \tag{20}$$

Note that the total degree of polarisation, $P = |\mathbf{P}|$, is unity in this case, i.e.

$$P^2 = {L_\perp}^2 + {P_\ell}^2 = 1\,, \tag{21}$$

indicating full coherence of the emitted radiation.

5. Generalised *STU* Parameters

Another way of obtaining information about the collision process, particularly with regard to spin-dependent effects, is the determination of the "generalised *STU* parameters" that describe the change of an arbitrary initial electron polarisation through scattering from unpolarised target atoms. The preparation of the projectile and target beams before the collision is identical to the electron–photon coincidence experiment with polarised electrons discussed above, but the photon detector and the coincidence unit for the detection of the final state are replaced by a Mott detector for the spin polarisation analysis of the scattered electrons.

The physical meaning of the generalised *STU* parameters is illustrated in Fig. 5. As discussed in detail in a previous review (Bartschat 1989), there are, in general, eight parameters that describe the reduced spin density matrix of the scattered projectiles completely. Besides the *absolute* differential cross section σ_u for the scattering of unpolarised electrons, there are seven *relative* generalised *STU* parameters: The polarisation function S_P determines the polarisation of an initially unpolarised projectile beam after the scattering, while the asymmetry function S_A determines the left–right asymmetry in the differential cross section for scattering of spin polarised projectiles. Furthermore, the contraction parameters T_x, T_y, T_z describe the change of an initial polarisation component along the three Cartesian axes, while the parameters U_{xy} and U_{yx} determine the rotation of a polarisation component in the scattering plane. Note that the number of independent *STU* parameters may be reduced in certain cases; the most important examples are (i) elastic scattering, (ii) transitions between target states without

angular momentum in both the initial and the final state, and (iii) situations where relativistic effects during the collision may be neglected (for further details see Bartschat 1989).

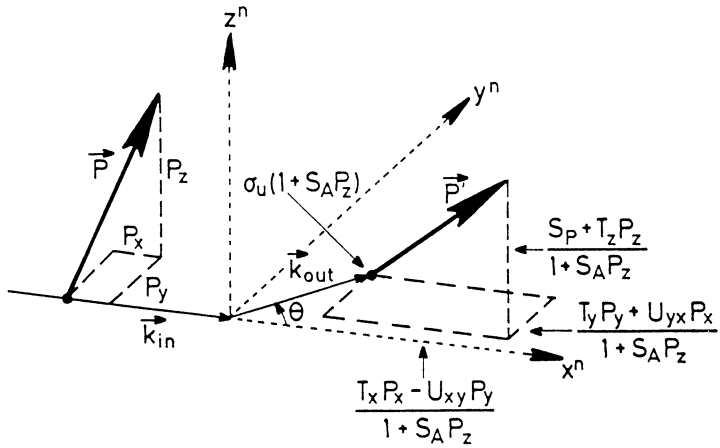

Fig. 5. Physical meaning of the generalised *STU* parameters for an initial spin polarisation **P** which is changed to a final spin polarisation **P′** through the scattering process (see text).

The concept of the generalised *STU* parameters can be extended in a systematic way to account for initially polarised targets and even a polarisation analysis of the target spin in the final state. Since such experiments have not been performed to date and are not expected to be performed in the near future (at least not for excitation processes), we only mention here one type of parameter that can provide important additional information. The general idea is shown in Fig. 6: one starts with both projectile and target beams spin-polarised, with polarisation vectors $\mathbf{P}_A = P_A\hat{\mathbf{x}}$ and $\mathbf{P}_B = P_B\hat{\mathbf{y}}$ orthogonal to each other; after the scattering, the polarisation component $P'\hat{\mathbf{z}}$ of the projectile beam *perpendicular* to the plane defined by the initial polarisation vectors is determined, and the result is normalised to the product of the initial polarisation magnitudes. We denote the corresponding parameter by the generic symbol V, i.e.

$$V = \frac{P'}{P_A\, P_B}\,. \tag{22}$$

It should be pointed out that many such independent V parameters can be defined, particularly in cases where relativistic effects and, consequently, the *relative orientation* of the scattering plane *and* the plane defined by the initial polarisation vectors must be taken into account.

6. Perfect Experiments

While perfect experiments for electron impact excitation of helium can be performed without considering the electron spin at all, it is interesting to note that neither the generalised Stokes nor the generalised *STU* parameters alone

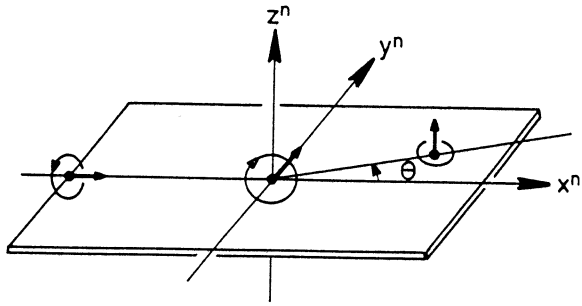

Fig. 6. Schematic diagram of an experiment to determine the rotation of an electron spin polarisation out of the plane spanned by orthogonal initial electron and atomic spin polarisations (see text).

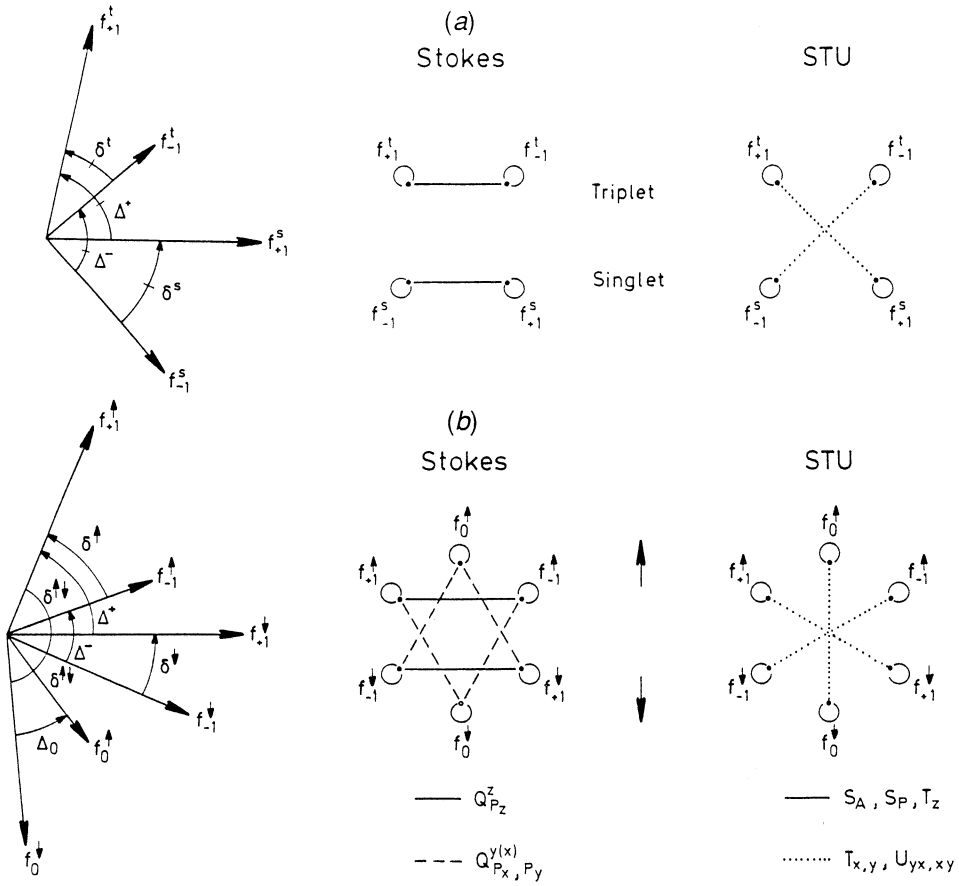

Fig. 7. Schematic diagram of independent amplitudes for S ⟶ P transitions. (*a*) Light alkali-type targets; (*b*) $J_0 = 0 \longrightarrow J_1 = 1$ transition in heavy targets. Also indicated are the relative amplitude sizes and phase angles that can be obtained from measurements of the generalised Stokes and *STU* parameters, respectively.

contain sufficient information to perform such an experiment for the other two cases (light alkalis and Hg $^3P_1$) discussed above.

The amount of information contained in the atomic density matrix (i.e. the Stokes parameters) and the reduced density matrix of the scattered electrons (i.e. the *STU* parameters) is illustrated in Fig. 7. For the alkali case (a), a Stokes parameter analysis provides information about the relative phase between the two f^t_{+1} and f^t_{-1} amplitudes and the relative phase between the two f^s_{+1} and f^s_{-1} amplitudes, as well as the relative sizes of all four amplitudes. For the mercury case (b), the fundamental difference between the information extracted from generalised Stokes and *STU* parameters can be summarised as follows (for details see Andersen *et al.* 1996*a*): A generalised Stokes parameter analysis in the $\mathbf{z}$ direction with electron spin polarisation $P_z\mathbf{z}$ perpendicular to the scattering plane gives information about all relative amplitude magnitudes, and the phase relationship between the f_{+1} and f_{-1} amplitudes. In addition, photon analysis in the $\mathbf{y}$ (or $\mathbf{x}$) direction with in-plane spin polarisation $P_y\mathbf{y}$ or $P_x\mathbf{x}$ yields the four relative phases within the two triples $(f^{\uparrow}_0, f^{\downarrow}_{+1}, f^{\downarrow}_{-1})$ and $(f^{\downarrow}_0, f^{\uparrow}_{+1}, f^{\uparrow}_{-1})$, respectively. None of the relative phases $(\Delta^+, \Delta^0, \Delta^-)$ between $f^{\uparrow}_{+1}$ and $f^{\downarrow}_{+1}$, etc. enter. It can also be shown (Andersen *et al.* 1996*a*) that the generalised *STU* parameters S_A, S_P and T_z are determined only by the relative sizes of the amplitudes, i.e. they can actually be predicted from generalised Stokes parameter measurements! Hence, such very different ways to measure the same physical observable can again be used as valuable consistency checks. Finally, T_x, T_y, U_{yx}, and U_{xy} also depend on the relative phases $(\Delta^+, \Delta^0, \Delta^-)$ *within* the three amplitude pairs $(f^{\uparrow}_{+1}, f^{\downarrow}_{+1})$, $(f^{\uparrow}_{-1}, f^{\downarrow}_{-1})$, and $(f^{\uparrow}_0, f^{\downarrow}_0)$. Since no information on the relative phase angles *between* these pairs can be extracted from a generalised Stokes parameter analysis, neither set alone will allow for a "perfect experiment", since at least one phase difference would be impossible to determine. A combination of experimental data for both parameters sets, however, allows for the determination of all magnitudes and relative phases, with many opportunities for valuable consistency checks.

We have recently demonstrated (see I) how a combination of data from different experiments would, in principle, have allowed for a "near perfect experiment" in electron–sodium excitation where only a few ambiguities would have remained in the signs of relative phases. The actual experimental setups are those for Stokes parameter analysis (or laser preparation) using unpolarised beams in Adelaide (Scholten *et al.* 1993) and spin-polarised beams at NIST (Kelley *et al.* 1992), and a T measurement with spin-polarised electrons by the Münster group (Hegemann *et al.* 1991, 1992). Unfortunately, data from all three experiments were not available at a single coinciding pair of energy and angle. We therefore demonstrated the principle by stimulating the procedure through combination with theoretical results from a "close-coupling plus optical potential" (CCO) calculation by Bray and McCarthy (1993). The results are shown in Fig. 8 for a total collision energy at $4{\cdot}1$ eV. The very good agreement between the actual and the "ghost" theoretical solutions with two sets of possible experimental data allows for a choice of the proper experimental result with a high degree of confidence. On a purely experimental basis, the remaining ambiguities could have been removed by using "in-plane" laser pumping in the NIST experiment and performing either a V or a fine-structure resolved U measurement.

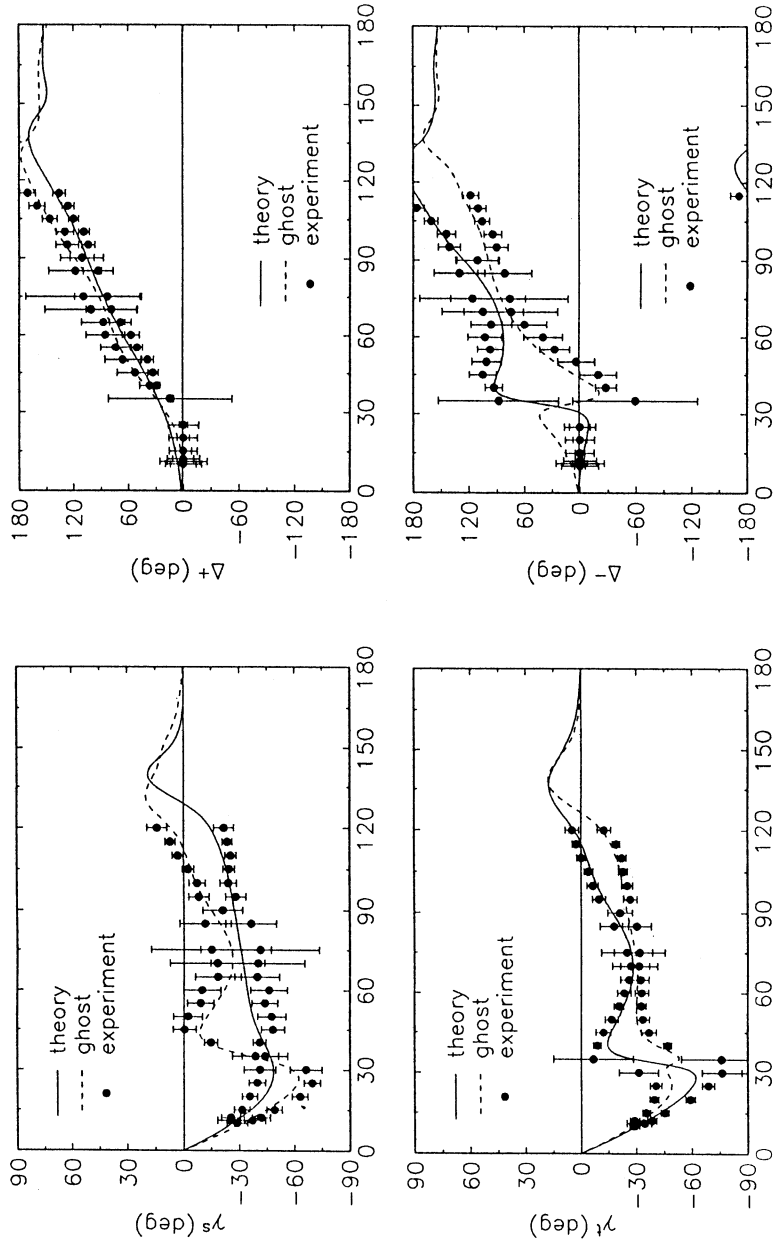

Fig. 8. Alignment angles γ^t and γ^s and singlet–triplet phase angles Δ^+ and Δ^- for electron impact excitation of the $3\,^2\mathrm{P}$ state of sodium at an incident electron energy of 4·1 eV. The "experimental" results were obtained through "inversion" of the NIST data (Kelley *et al.* 1992) for $(r, L_\perp^t, L_\perp^s)$, supplemented by theoretical CCO results of Bray and McCarthy (1993). ●, two sets of inverted experimental data as well as the true (——) and one ghost (– – –) solution. (For more details see I.)

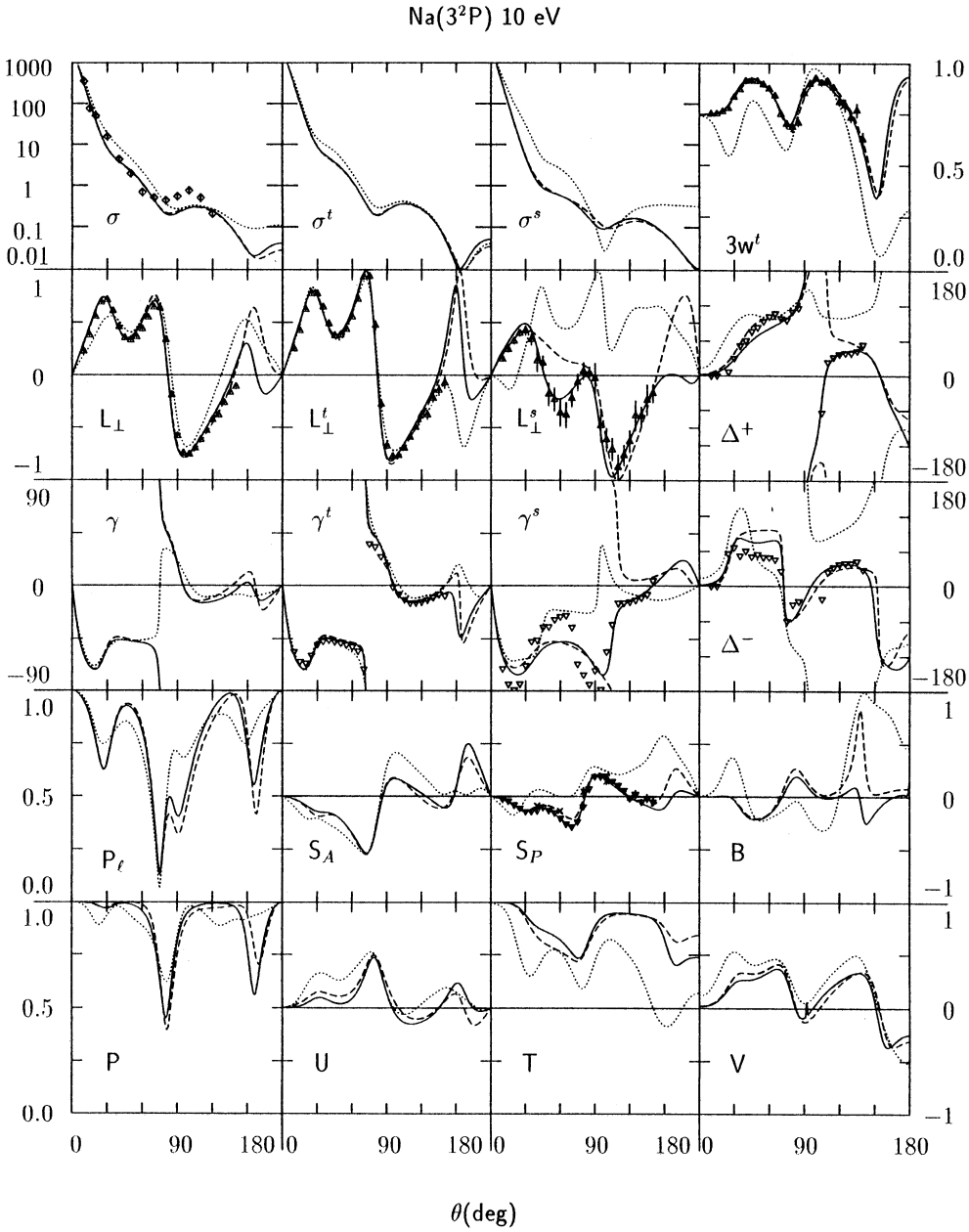

Fig. 9. Survey of alignment and orientation parameters for excitation of the Na $3\,^2P$ state by spin-polarised electrons at a total collision energy of 10·0 eV. The experimental data are from: ◇, Srivastava and Vuskovic (1980); △, Kelley *et al.* (1992); ×, Nickich *et al.* (1990); and ▽, "inverted" NIST data (see text). Theoretical curves represent: ——, CCC of Bray (1994); -----, CCO of Bray and McCarthy (1993); and ·····, DWB2 of Madison *et al.* (1992).

7. Example Results

Fig. 9 displays an overview of spin-resolved alignment and orientation parameters for electron impact excitation of the $(3s)^2S \longrightarrow (3p)^2P$ transitions in sodium at an incident electron energy of 10 eV, as well as some generalised *STU* parameters. The latter are for the $(3p)^2P_{1/2}$ fine-structure level; assuming that relativistic effects can be neglected, these parameters are trivially related to those for the $^2P_{3/2}$ state (for details, see I).

It can be seen that the "close-coupling plus optical potential" (CCO) method of Bray and McCarthy (1993), and particularly the more recent "convergent close-coupling" (CCC) approach of Bray (1994), yields theoretical results that are in excellent agreement with the available experimental data, most of which were obtained in the superelastic setup of the NIST group (for a summary see Kelley *et al.* 1992). Note in particular that only the CCC theory is able to reproduce the experimental data for the angular momentum transfer $L_\perp^s$ in the singlet channel. While the second-order distorted-wave (DWB2) results of Madison *et al.* (1992) are in good agreement with the close-coupling predictions and experiment for some of the parameters, large discrepancies remain for others. Not surprisingly, this indicates that perturbation theory, even to second order, is not sufficiently accurate at this low collision energy. We also note that the "experimental" $\gamma^{s,t}$ and the $\Delta^{\pm}$ angles shown in Fig. 9 were obtained by combining data from various experiments and using theory to choose a particular set, thereby "eliminating" the remaining ambiguities (see the previous section and I for more details).

Given the success of the theoretical approaches for the electron–sodium collision system, the discrepancies between theoretical predictions and experimental data for electron impact excitation of hydrogen at 54·4 eV total collision energy (see Fig. 10) seem very surprising. Theoretical results obtained with both non-perturbative close-coupling and perturbative (second-order) methods agree with each other much better than with two sets of independent experimental data. In most cases, however, the data from the different experiments also agree with each other within the specified error bars. In light of recent technological advances, theorists have frequently called for new measurements which, especially when spin-resolved, may either eliminate or at least shine more light on these discrepancies. While spin-resolved measurements seem very desirable, we point out that the theoretical predictions for alignment and orientation parameters in the two spin channels are very similar at 54·4 eV and, therefore, close to the spin-averaged results. This is due to the fact that electron exchange processes are not very likely at such a high collision energy, thereby causing singlet and triplet amplitudes to be very similar as well.

As the last example, Fig. 11 displays some generalised Stokes parameter matrix elements for electron impact excitation of the $(6s^2)^1S_0 \rightarrow (6s6p)^3P_1$ transition in Hg by spin-polarised electrons. These were derived from raw experimental data of Goeke *et al.* (1989) and of Sohn and Hanne (1992). They are compared with theoretical results based on a five-state Breit–Pauli R-matrix calculation (Scott *et al.* 1983; Bartschat *et al.* 1984). The agreement between the experimental data and the theoretical predictions is satisfactory, keeping in mind the complexity of the collision problem and the level of detail in the comparison. Note that the experimental data for $\left(Q_{13}^{\hat{\mathbf{z}}}\right)_{P_z}$, $\left(Q_{23}^{\hat{\mathbf{z}}}\right)_{P_z}$ and $\left(Q_{33}^{\hat{\mathbf{z}}}\right)_{P_z}$, which should be identical within the error bars, are not completely consistent, although a tendency towards

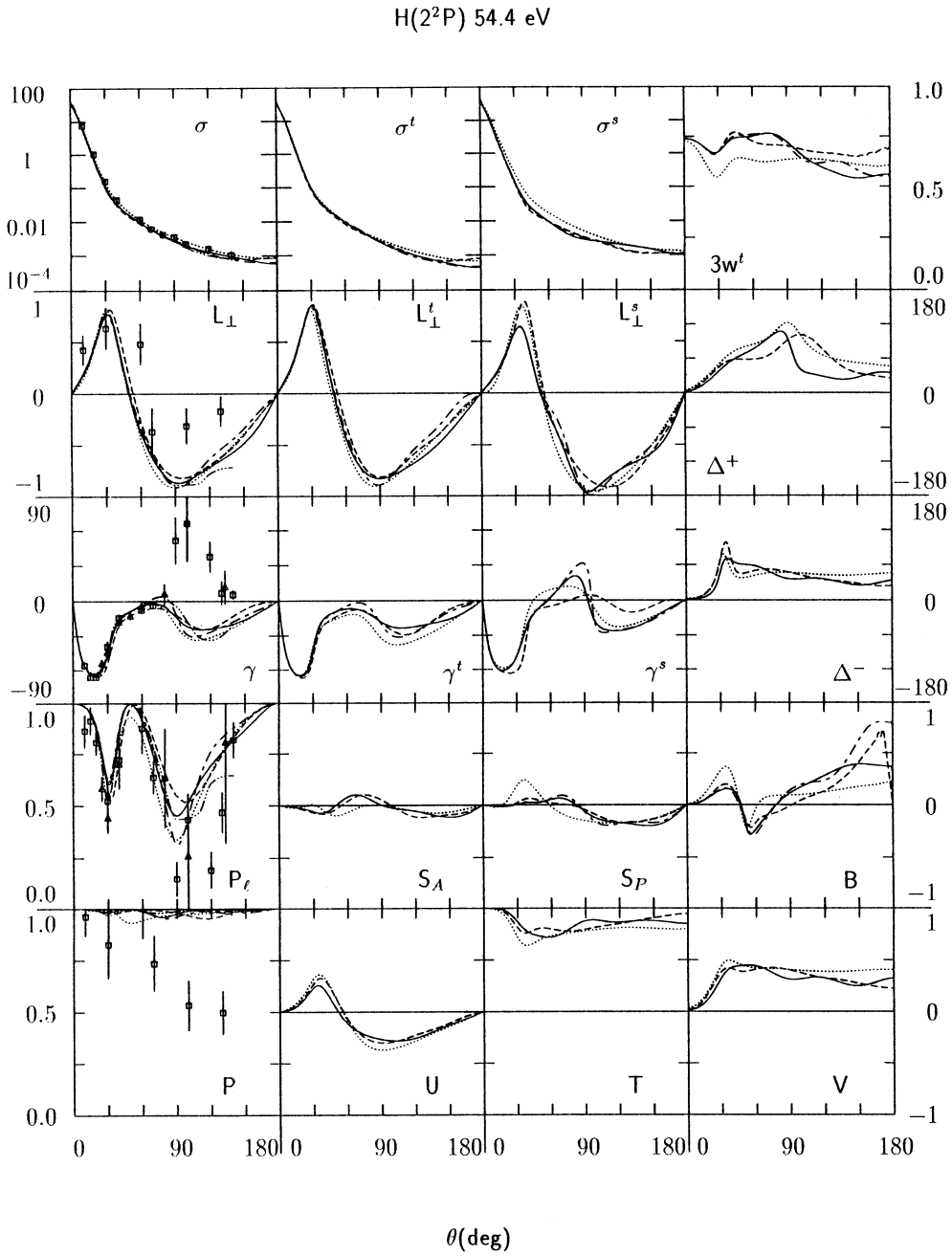

Fig. 10. Survey of alignment and orientation parameters for excitation of the H $2\,^2$P state by spin-polarised electrons at a total collision energy of 54·4 eV. The experimental data are from: △, Weigold *et al.* (1980); and □, Williams (1981, 1986). Theoretical curves represent: ——, CCC of Bray and Stelbovics (1992); - - - - -, CCO of Bray *et al.* (1991); — - —, intermediate energy *R*-matrix method of Scholz *et al.* (1991); — · · —, pseudo-state close-coupling approach of Van Wyngaarden and Walters (1986); and · · · · · ·, DWB2 of Madison *et al.* (1991).

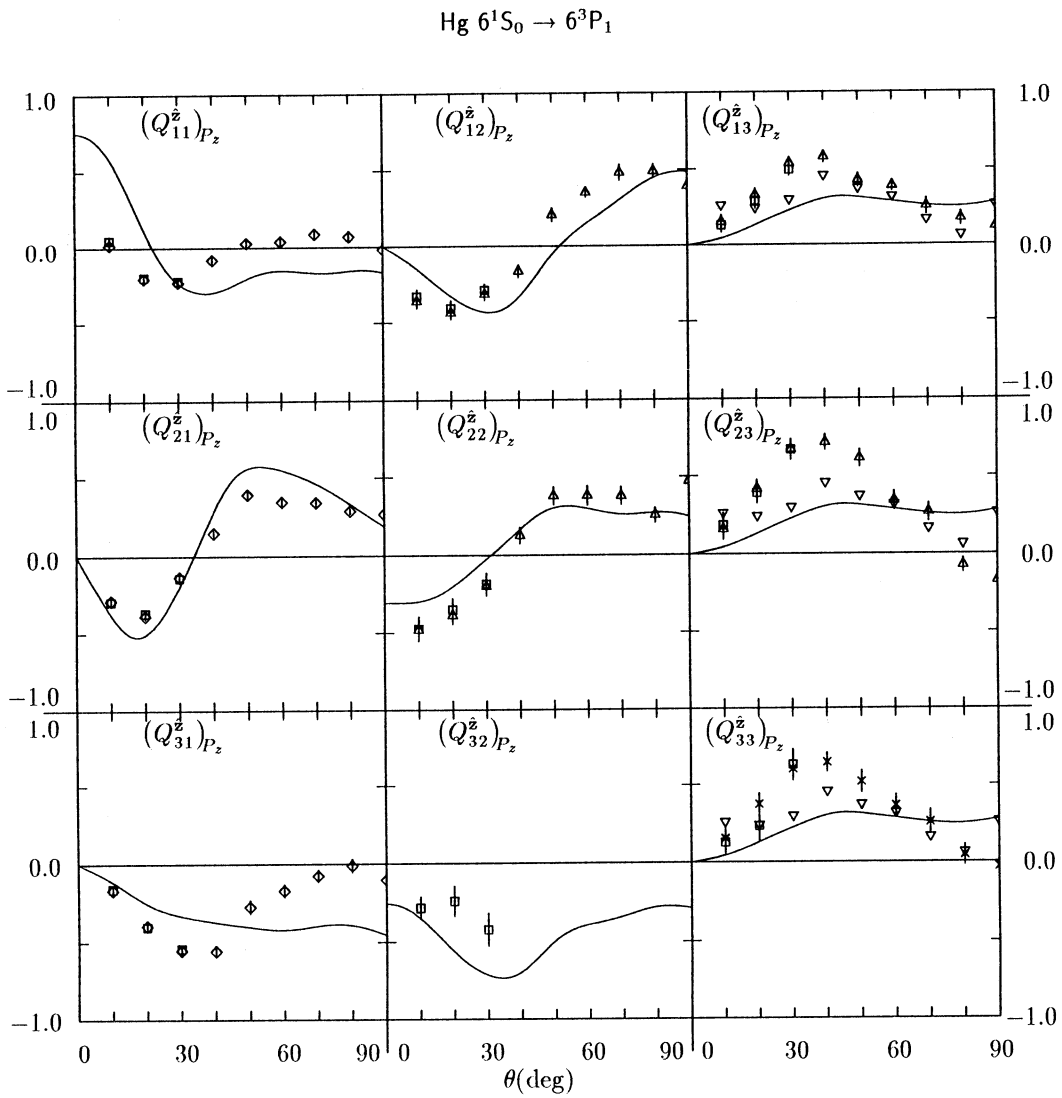

Fig. 11. Generalised Stokes parameters for electron impact excitation of Hg(6s6p)^{3}P$_1$ at an incident electron energy of 8 eV. ◇, measured data of Goeke *et al.* (1989) and of Sohn and Hanne (1992); □, unpublished data of Sohn and Hanne (1992); △, calculated from experimental raw data; ▽, prediction based on properties of the generalised Stokes parameters (see text); and ×, consistency check using an alternative prediction based on properties of the generalised Stokes parameters (for details see Andersen *et al.* 1996*a*). The experimental results are compared with the predictions from a five-state Breit–Pauli *R*-matrix calculation based on the work of Scott *et al.* (1983) and of Bartschat *et al.* (1984).

the same results is recognised. After tedious algebraic manipulations, we have also extracted spin-resolved alignment and orientation parameters from these data which lead to interesting conclusions about the validity of propensity rules. The results will be presented elsewhere (Andersen *et al.* 1996*b*).

8. Summary and Outlook

In this paper, we have outlined how spin-resolved orientation and alignment parameters allow for a very detailed test of theoretical models. They can

be extracted from measurements of "generalised Stokes parameters" and, when combined with data for the absolute differential cross section σ_u and the relative "generalised STU parameters", consist of a "perfect experiment" where all the magnitudes and relative phases of the individual scattering amplitudes are determined. Except for the helium target, such experiments have not been reported for excitation to date, but they can be performed with presently existing experimental setups. The complexity of the problem, however, calls for *increased coordination* of efforts by different experimental groups, as well as careful consistency checks between the raw data.

We believe that further experimental work is needed for the fundamental problem of electron scattering from atomic hydrogen, where spin-resolved work may give hints about the origin of the remaining discrepancies between experimental data and theoretical predictions. Another system, for which a complete experiment is within reach, is low-energy electron impact excitation of mercury. Here spin-resolved alignment and orientation data could not only provide benchmark tests for theoretical approaches, but also reveal important information about propensity rules and their applicability to spin-resolved collision processes.

Acknowledgments

We wish to thank Igor Bray, Friedrich Hanne, Mike Kelley, Don Madison, Jabez McClelland and Peter Teubner for readily communicating their data in numerical form, and John Broad and Jean Gallagher for providing financial support and excellent working conditions at the JILA Data Center where these ideas matured. This work was also supported by the United States National Science Foundation (KB) and by the Danish Natural Science Research Council (NA).

References

Andersen, N., and Bartschat, K. (1993). *Comm. At. Mol. Phys.* **29**, 157.
Andersen, N., and Bartschat, K. (1994). *J. Phys.* B **25**, 3189.
Andersen, N., Bartschat, K., Broad, J. T., and Hertel, I. V. (1996*a*). *Phys. Rep.* (in press).
Andersen, N., Bartschat, K., Broad, J. T., Hanne, G. F., and Uhrig, M. (1996*b*). *Phys. Rev. Lett.* (in press).
Andersen, N., Gallagher, J. W., and Hertel, I. V. (1988). *Phys. Rep.* **165**, 1.
Bartschat, K. (1989). *Phys. Rep.* **180**, 1.
Bartschat, K., Blum, K., Hanne, G. F., and Kessler, J. (1981). *J. Phys.* B **14**, 3761.
Bartschat, K., Scott, N. S., Blum, K., and Burke, P. G. (1984). *J. Phys.* B **17**, 260.
Becker, K., Crowe, A., and McConkey, J. W. (1992). *J. Phys.* B **25**, 3885.
Bederson, B. (1970). *Comm. At. Mol. Phys.* **2**, 160.
Blum, K. (1981). 'Density Matrix Theory and Applications' (Plenum: New York).
Bray, I. (1994). *Phys. Rev.* A **49**, 1066.
Bray, I., Konovalov, D. A., and McCarthy, I. E. (1991). *Phys. Rev.* A **44**, 5586.
Bray, I., and McCarthy, I. E. (1993). *Phys. Rev.* A **47**, 317.
Bray, I., and Stelbovics, A. T. (1992). *Phys. Rev.* A **46**, 6995.
Goeke, J., Hanne, G. F., and Kessler, J. (1988). *Phys. Rev. Lett.* **61**, 58.
Goeke, J., Hanne, G. F., and Kessler, J. (1989). *J. Phys.* B **22**, 1075.
Hegemann, T., Oberste-Vorth, M., Vogts, R., and Hanne, G. F. (1991). *Phys. Rev. Lett.* **66**, 2968.
Hegemann, T., Schroll, S., and Hanne, G. F. (1992). *J. Phys.* B **26**, 4607.
Hertel, I. V., Kelley, M. H., and McClelland, J. J. (1987). *Z. Phys.* D **6**, 163.
Kelley, M. H., McClelland, J. J., and Lorentz, S. R., Scholten, R. E., and Celotta, R. J. (1992). *In* 'Correlation and Polarisation in Electronic and Atomic Collisions and (e,2e) Reactions' (Eds P. J. O. Teubner and E. Weigold), p. 23 (Institute of Physics: Bristol).

Kessler, J. (1985). 'Polarised Electrons' (Springer: New York).
Madison, D. H., Bartschat, K., and McEachran, R. P. (1992). *J. Phys.* B **25**, 5199.
Madison, D. H., Bray, I., and McCarthy, I. E. (1991). *J. Phys.* B **24**, 3861.
McClelland, J. J., Kelley, M. H., and Celotta, R. J. (1985). *Phys. Rev. Lett.* **55**, 688.
McClelland, J. J., Kelley, M. H., and Celotta, R. J. (1989). *Phys. Rev.* A **40**, 2321.
Nickich, V., Hegemann, T., Bartsch, M., and Hanne, G. F. (1990). *Z. Phys.* D **16**, 261.
Pierce, D. T., Celotta, R. J., Wang, G.-C., Unertl, W. N., Galejs, A., and Kuyatt, C. E. (1980). *Rev. Sci. Instrum.* **51**, 478.
Scholten, R. E., Shen, G. F., and Teubner, P. J. O. (1993). *J. Phys.* B **26**, 987.
Scholz, T. T., Walters, H. R. J., Burke, P. G., and Scott, M. P. (1991). *J. Phys.* B **24**, 2097.
Scott, N. S., Burke, P. G., and Bartschat, K. (1983). *J. Phys.* B **16**, L361.
Sohn, M., and Hanne, G. F. (1992). *J. Phys.* B **25**, 4627.
Srivastava, S. K., and Vuskovic, L. (1980). *J. Phys.* B **13**, 2633.
Van Wyngaarden, W. L., and Walters, H. R. J. (1986). *J. Phys.* B **19**, 1827.
Weigold, E., Frost, L., and Nygaard, K. J. (1980). *Phys. Rev.* A **21**, 1950.
Williams, J. F. (1981). *J. Phys.* B **14**, 1197.
Williams, J. F. (1986). *Aust. J. Phys.* B **39**, 621.

Manuscript received 15 February, accepted 2 May 1995